Dental Materials xxx (xxxx) xxx

Contents lists available at ScienceDirect

Dental Materials

journal homepage: www.elsevier.com/locate/dental

Edge strength of definitive 3D-printed restorative resin materials

Shaymaa Mudhaffer [a,b,*], Julfikar Haider [a,c], Nick Silikas [a], Julian Satterthwaite [a]

[a] Division of Dentistry, School of Medical Sciences, University of Manchester, Manchester, UK
[b] Substitutive Dental Sciences, Faculty of Dentistry, Taibah University, Madinah, Saudi Arabia
[c] Department of Engineering, Manchester Metropolitan University, Manchester, UK

ARTICLE INFO

Keywords:
Resin composite
3D printing
Additive manufacturing
Subtractive manufacturing
Edge strength
Definitive resins
Interim resins

ABSTRACT

Statement of the problem: With the advent of digital technology in dentistry, manual methods for creating dental restorations are being replaced by digital CAD/CAM processes involving three-dimensional (3D) printing and milling. Marginal degradation and chipping are common issues, yet the literature on the edge strength of 3D-printed restorative materials remains limited. Uncertainties remain regarding the impact of print orientation on edge strength, necessitating further investigation to ensure clinical efficacy.

Purpose: The purpose of this study was to evaluate the influence of print orientation on the edge strength of 3D-printed dental restorative resins indicated for definitive and interim use and compare them with milled materials.

Materials and methods: Specimens (14 ×14 ×2 mm) were additively manufactured in three orientations (0, 45, and 90 degrees) using five 3D printed resins: VarseoSmile Crown^{plus} (VCP), Crowntec (CT), Nextdent C&B MFH (ND), Dima C&B temp (DT), and GC temp print (GC). A DLP 3D printer (ASIGA MAX UV) was used, with post-processing parameters set according to manufacturer recommendations. Edge strength was measured at 0.5 mm and 1 mm distance from the edge using a CK 10 testing machine. Specimens were tested in dry conditions (0.5 mm) and after 48 hours of storage in artificial saliva at 37°C (0.5 mm and 1 mm). Failure modes were analysed visually and using optical and scanning electron microscopy. Filler content was assessed using the Ash method, and statistical analysis was conducted using ANOVA. Pearson correlation was used to assess the relationship between filler weight and edge strength.

Results: Due to severe deformation before chipping under load at both distances, data for the 3D-printed and milled interim materials were excluded. The 90-degree printing orientation of definitive materials demonstrated significantly higher edge strength after 48 hours in artificial saliva compared to the 0- and 45-degree orientations ($P < 0.001$). Significant differences were observed between the 3D printed and milled materials at 0.5 ($P < 0.001$) mm but not at 1 mm ($P \geq 0.804$). Failure modes were predominantly surface indentation without visible cracking (58 %), followed by surface indentation with visible cracking (17 %), edge chipping (0.2 %), and specimen fracture (13 %). A non-significant negative correlation was observed between filler weight and edge strength ($r = 0.161$, $P < 0.680$).

Conclusions: Based on the current findings, 3D printing definitive resin materials at a 90-degree orientation provided increased edge strength. 3D-printed materials can better resist crack propagation compared to milled composites.

Clinical implications: Optimizing the print orientation to 90-degree can improve the edge strength of definitive 3D printed materials.

1. Introduction

With the advancement of digital technology in dentistry, traditional manual methods for creating dental restorations are giving way to digital CAD/CAM manufacturing processes, which are now widely embraced in dental laboratories [1]. These processes involve two main techniques: subtractive manufacturing (SM), which entails milling from a solid block, and additive manufacturing (AM), also known as three-dimensional (3D) printing [2]. Unlike SM, AM offers the advantage of producing objects with intricate geometries while minimizing material loss and avoiding wear of rotary tools [3,4]. Among 3D printing technologies, digital light processing (DLP) is notable for printing dental

* Correspondence to: Division of Dentistry, School of Medical Sciences, University of Manchester, Coupland 3 Building, Oxford Road, Manchester M13 9PL, UK.
E-mail address: Smudhaffer@Taibahu.edu.sa (S. Mudhaffer).

https://doi.org/10.1016/j.dental.2025.04.005
Received 9 December 2024; Received in revised form 26 March 2025; Accepted 15 April 2025
Available online 18 April 2025

prostheses, utilizing UV polymerization of photosensitive resin-based materials to construct objects layer by layer [5,6]. This layer-based manufacturing process results in anisotropic objects, where the properties of the printed fixed dental prosthesis can vary depending on the building direction [7–9]. While optical [10], surface [11,12], and mechanical properties, such as flexural strength [13,14], and hardness [15,16], have been examined, literature on the edge strength of 3D printed restorative material is limited.

Marginal degradation and chipping are common mechanical issues encountered in fixed dental prosthesis subjected to excessive masticatory forces [17]. Clinically, restoration chipping can lead to various adverse outcomes, such as marginal discoloration, compromised aesthetics, plaque accumulation at fractured edges, and an increased risk of secondary caries, especially in hard-to-reach areas with inadequate oral hygiene [17,18]. Brittle materials, such as composite resins, are prone to cracking, chipping, or fracturing at the margins or cusps, which weakens the restoration and may lead to its complete failure. While minor chips can sometimes be repaired, more severe cases often necessitate full replacement of the restoration, resulting in further loss of natural tooth structure [19,20].

Marginal integrity and fracture resistance of restorative materials are essential for the long-term success of any restoration [21]. However, ensuring adequate marginal integrity remains a significant clinical challenge, as restorations are more prone to chipping near the edges [22]. Chipping can occur at a crown margin during manufacturing and can dramatically weaken the restoration. Major cracks can emanate from these marginal chips and compromise the restoration's overall strength [22].

To address these clinical challenges, an edge strength test is commonly used to evaluate the marginal stability of a restoration [23].

Table 1
Material composition provided by their manufacturers.

	Material	Manufacturer	Composition	%(w/w)	Lot. #	Shade	Indications
Additive	**Varseosmile Crown^{plus} (VCP)**	BEGO, Germany	Esterification products of 4.4′-isopropylidiphenol, ethoxylated and 2-methylprop−2enoic acid	50–75	600414	A2	Definitive crowns, inlays, onlays, and veneers
			Silanized dental glass (particle size 0.7 μm)	30–50			
			Diphenyl (2,4,6-trimethylbenzoyl) phosphine oxide	< 2.5			
			Methyl benzoylformate	-			
	Crowntec (CT)	Saremco Dental AG, Switzerland	Bis-EMA	50–75	D937	A2	Definitive crowns, inlays, onlays, veneers, denture teeth and temporary bridges.
			Trimethylbenzonyldiphenyl phosphine oxide	0.1 - < 1			
			Silanized dental glass, pyrogenic silica (particle size 0.7 μm)	30–50			
			Catalyst and Inhibitors	-			
	NextDent C&B MFH (ND)	3D systems, Netherlands	7,7,9(or 7,9,9)-trimethyl−4,13-dioxo−3,14-dioxa−5,12-diazahexadecane−1,16-diyl bismethacrylate	50–75	WX495N02	N1	Crowns and bridges for long term interim use
			2-hydroxyethyl methacrylate	< 25			
			Ethoxylated bisphenol A dimethacrylate	< 10			
			Ethylene dimethacrylate	< 10			
			Silicon dioxide	1–5			
			Diphenyl (2,4,6-trimethylbenzoyl) phosphine oxide	1–5			
			Mequinol; 4-methoxyphenol; hydroquinone monomethyl ether	< 0.1			
			Titanium dioxide	< 0.1			
	Dima C&B temp	Kulzer, Germany	Esterification products of 4,4′-isopropylidiphenol, ethoxylated and 2-methylprop−2enoic acid	40–60	CD21G06A35	A2	Interim crowns or bridges up to 1 year
			7,7,9(or 7,9,9)-trimethyl−4,13-dioxo−3,14-dioxa−5,12- diazahexadecane−1,16-diyl bismethacrylate	30–50			
			Propylidynetrimethyl trimethacrylate	3–10			
			Diphenyl (2,4,6-trimethylbenzoyl) phosphine oxide	< 3			
			Mequinol	< 1			
	GC temp print (GC)	GC dental, Japan	UDMA	50–75	2206101	A2	Long term interim crowns, bridges, inlays, onlays and veneers
			2,2′-ethylenedioxydiethyl dimethacrylate	10-< 25			
			Esterification products of 4,4′-isopropylidenediphenol, ethoxylated and 2-methylprop2-enoic acid	2.5-< 5			
			Quartz (silicon dioxide)	10-< 25			
			Diphenyl (2,4,6-trimethylbenzoyl) phosphine oxide	< 2.5			
			2-(2H-benzotriazol−2-yl)-p-cresol	0.1-< 0.2			
Subtractive	**Lava Ultimate (LU)**	3 M ESPE, USA	BisGMA, UDMA, BisEMA, TEGDMA	20	NC95259	A2	Definitive inlays, onlays and veneers
			Silica nanomers (20 nm)	80			
			Zirconia nanomers (4–11 nm)				
			Silica-zirconia nanoclusters (0.6–10 μm)				
	Telio CAD (TC)	Ivoclar vivadent AG,	Polymethyle methaacrylate	99.5	Z02TYX		Interim crowns, interim bridges and implant supported interim crowns
			Pigments	< 1			

Fracture and chipping are reported to be influenced by the distance from the edge, the thickness of the restoration, the type of intender, and bonding to the underlying structure [20,24]. Watts et al. [25,26] have characterized edge strength as the force required to make a chip at 0.5 mm from the edge, which is thought to be clinically relevant to the marginal breakdown of restorations.

The force required to create a chip has been reported to increase linearly with increasing distance from the edge [20,27]. However, However, nonlinear behaviour has also been observed in soft dental restorative materials [27]. While a full characterization is best achieved by collecting data over a broad range of forces and distances, a simple material comparison can be conducted at a 0.5 mm distance from the edge, representing edge strength [24]. This test holds clinical relevance as chips mimic clinical failures, and the shape and size of the chips can provide valuable clinical insights [17,22,24]. While initially established for brittle materials, this method has since been adapted for polymethyl methacrylates and composite resins [27].

The objectives of this study were: (i) To evaluate the effect of printing orientation on the edge strength, (ii) To determine the edge strength of different 3D printed and milled definitive resin materials.

The null hypotheses tested were: (i) There is no difference in the edge strength between 0, 45, and 90-degree printing orientations of 3D printed resin materials. (ii) There is no difference in the edge strength between 3D printed and milled materials indicated for definitive and interim applications. (iii) The force required to create a chip does not increase with increasing distance from the edge. (iv) No correlations exist between filler weight and edge strength of the different tested materials.

2. Materials and methods

2.1. Materials and specimen preparation

Five 3D printed resin materials and two milled materials used in this study are presented in Table 1. A specimen measuring 14 × 14 × 2.3 mm was designed using a free online software (Tinkercad) then exported as an STL file and imported into CAM software, Composer (version 1.3.2, 2021, ASIGA). The printing parameters were adjusted, including orientation (0, 45, and 90 degree) (n = 20 for 0 and 45 degrees, n = 30 for 90 degrees), layer thickness (50 μm), specimen placement on the build platform, and support design (automatic configuration). The specimens were 3D printed using an ASIGA MAX UV 3D printer (ASIGA), which is an open system printer utilizing DLP technology with a light wavelength of 385 nm. After printing was completed, the specimens underwent a 5-minute cleaning process in 98 % ethanol (Sigma Aldrich) using Form Wash (Formlabs Inc.) and were left to air dry for 5 minutes. Support structures were then removed using a scalpel, and the specimens were post-polymerized in a light-curing unit according to manufacturer recommendations for each material (Table 2). Specimens from subtractive CAD/CAM blocks, Lava Ultimate and Telio CAD, were cut into sections (14 ×14 ×2.3 mm) using a diamond blade (MK 303; MK Diamond) mounted on a saw (Isomet 1000 Precision Saw; Buehler) with continuous water supply.

All 3D printed and milled specimens were polished using 800-grit silica carbide paper (Metaserve 250 grinder-polisher; Buehler) under continuous water cooling for 20 seconds on each side to ensure the surface was flat and smooth. Specimen thickness was verified with an electronic digital calliper (PDC150M, Draper Tools Ltd) ensuring an accuracy of ±0.1 mm and the final specimen dimension was 14 × 14 × 2 mm.

Specimens were randomly divided into two groups according to storage conditions: dry storage or wet storage in artificial saliva at 37°C for 48 hours. Fig. 1 describes the study design. Artificial saliva (AS) was prepared by dissolving sodium chloride (0.4 g), potassium chloride (0.4 g) calcium chloride (0.795 g), sodium dihydrogen phosphate (0.69 g), and sodium sulphide hydrate (0.005 g) in 1000 ml of distilled water [28,29]. The pH of AS was found to be 6.35 using a digital microprocessor pH meter (Mettler Toledo, model DELTA 340).

Table 2
Post curing device parameters and curing parameters for the 3D-printed resin materials.

Post curing device	Form cure	Otoflash G171	Cara print LED cure
Manufacturer	Formlabs, USA	NK-Optik, Germany	Kulzer, Germany
Light source	Light-emitting diode (LED)	Flashlight	LED
Light spectrum (wavelength)	405 nm	250–950 nm	370–470 nm
Maximum temperature	60–80 °C	n/a	30–80 °C
Materials and Curing recommendation	Nextdent C&B MFH (60°C for 30 min)	Varseosmile Crown^{plus} (2 ×1500 flashes) Crowntec (2 ×2000 flashes) GC Temp Print (2 ×400 flashes)	Dima C&B Temp (60°C for 20 min)

2.2. Edge strength testing

Edge-strength was measured using a CK 10 testing machine (Engineering systems) equipped with a polycrystalline 120° Rockwell C diamond indenter. This device has an integrated acoustic sensor to detect signals indicative of cracking or chipping. Each specimen was securely positioned on the X–Y table base, the table was then moved to locate the sample edge, the x-axis was zeroed and then the indenter was moved to the desired distance from the edge. Subsequently, the sample underwent compressive loading at a crosshead speed of 1 mm/min until failure. Four measurements were taken per sample (one measurement at each edge). In case of specimen fracture preventing further testing on the specimen, a minimum of 2 measurements was obtained. A total of 10 measurements were recorded for each subgroup (n = 10). All groups were tested at 0.5 mm distance from the edge. One group (90 degrees) was also tested at an additional 1 mm distance to evaluate force vs. distance relationship.

2.3. Failure analysis

Samples were examined visually to determine the mode of failure which was classified into four categories with increasing severity [30]:

1. Surface indentation without visible cracking.
2. Surface indentation with visible cracking.
3. Chipping: an edge fragment chipped off.
4. Fracture: total fracture of the specimen.

Additional images were captured using an optical microscope at 4x magnification (Echo, Revolve, USA), along with scanning electron microscope (SEM) images using the TM4000PLUS II Tabletop Microscope (Hitachi High-Tech Europe GmbH, Germany) with an SE detector, operating at 15 kV in low vacuum and 30x magnification. These images were used to explore undetected cracks and chipped edges.

2.4. Filler content assessment

The Ash method [31] was used to assess the filler weight proportion. Three samples of each material (n = 3) at a 0-degree orientation were printed and prepared as described in 2.1. Each specimen was subjected to 600°C for 30 minutes in an electric furnace (Programat EP 5000; Ivoclar Vivadent) to eliminate the organic component. They were left to

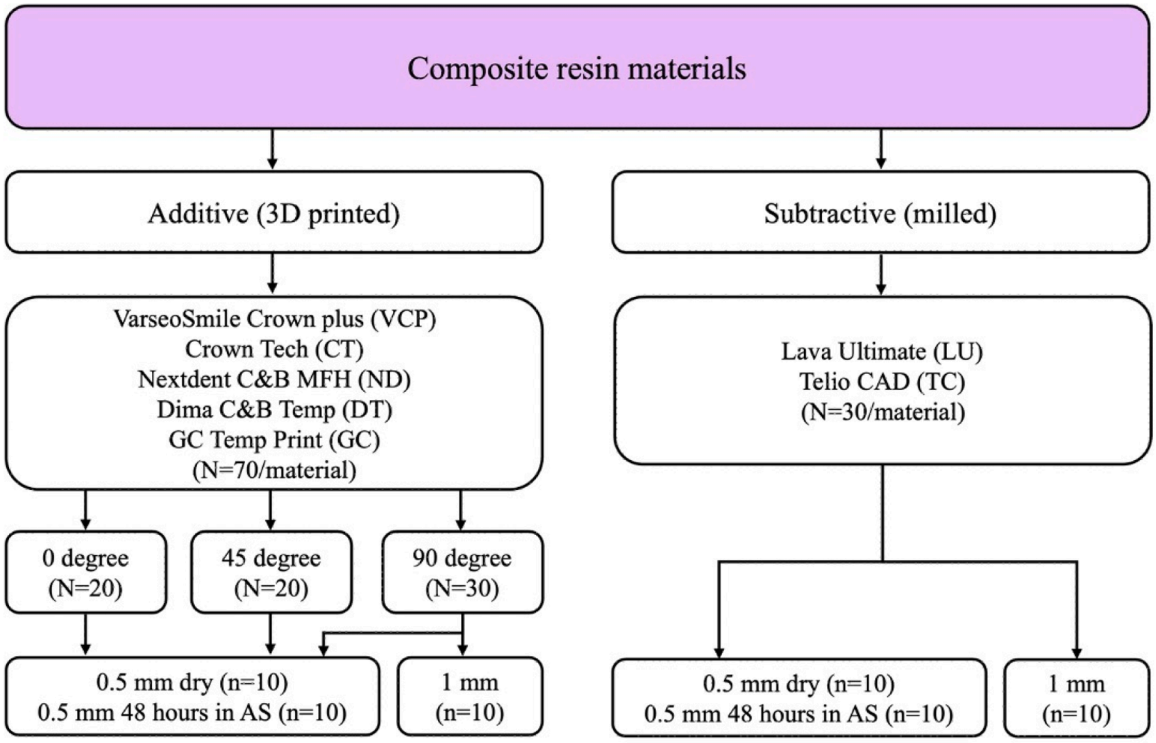

Fig. 1. Study design.

cool down completely then weighed using an electronic analytical balance, ensuring precision to 0.01 mg (Ohaus Analytical Plus; Ohaus Corporation). The percentage of inorganic filler weight was then calculated from:

$$\textit{Filler weight}.\% = ((w_3 - w_1))/((w_2 - w_1)) \times 100 \quad (1)$$

where w_1 is the initial mass of the dry crucible, w_2 is the initial mass of dry crucible combined with the dried sample, and w_3 is the final mass of the crucible combined with the sample residue.

2.5. Statistical analysis

Data analysis was conducted using a statistical software package (IBM SPSS Statistics, v29.0; IBM Corp). To assess variance normality and homogeneity, Shapiro-Wilk and Levene's tests were applied, respectively. A multiple-way ANOVA was executed to explore the interactions among the material groups and print orientations. One-way ANOVA, and Tukey's Post-Hoc test ($P \leq 0.05$) were employed to detect the interactions both within and between these variables. T-test was performed to investigate the difference between the storage conditions. Pearson correlation was used to explore the correlation between filler weight and ES (α=0.05 for all tests).

3. Results

3.1. Edge strength

All interim materials showed severe deformation before chipping at both distances (Fig. 2) and did not crack until after exhausting the elastic deformation limit. Thus, the data for the 3D printed and milled interim materials were not presented. Means and standard deviations of edge forces for the definitive materials are presented in Table 3 and Fig. 3.

A significant main effect was observed for material (η_p^2=0.357, $P < 0.001$), followed by orientation (η_p^2=0.091, $P < 0.001$). The interaction between material and orientation was also significant (η_p^2=0.134, $P < 0.001$).

In dry conditions, no differences were found between orientations for both materials ($P \geq 0.077$). After 48 hours in AS, specimens with a 90-degree orientation showed higher edge strength than those with 0- and 45-degree orientations ($P < 0.001$). Edge strength for all groups, except VCP 90-degree, decreased after 48 hours of storage compared to dry specimens, but this decrease was not statistically significant ($P \geq 0.082$)

Significant differences were observed in the edge strength between the definitive 3D printed and milled materials at 0.5 mm ($P < 0.001$) but not at 1 mm ($P \geq 0.804$). Edge strength for all materials increased as the distance of loading from the edge increased to 1 mm this increase was statistically significant ($P \leq 0.03$).

3.2. Observation on the modes of failure

Failure modes revealed by edge testing are detailed in Fig. 4. The main mode of failure was indentation without visible cracks (58 %), indentation with visible cracks (17 %), edge chipping (0.2 %), and fracture of the specimen (13 %).

All failure modes were observed in all materials except for VCP, where no chipping was observed. No chipping was observed at 1 mm distance from the edge for all materials. Indentations with visible cracks and fractures increased with increasing distance.

The predominant failure mode for the definitive 3D-printed group was indentation without visible cracks (Fig. 5). The indentation was shallow and barely visible. A blue felt tip marker was used to stain the edges in order to reduce internal reflections and to highlight topographical and fractographic features [27] and some cracks became visible after staining (Fig. 5). Indentation with visible cracks (Fig. 6) and chipping (Fig. 7) were also noticed. There was no consistent trend or pattern for crack propagation and there was no difference in failure mode between orientations of the same material. For the samples that chipped, chipping was either as a single piece or multiple pieces from the edge. Specimen fracture resulted in the specimens breaking into two or more pieces.

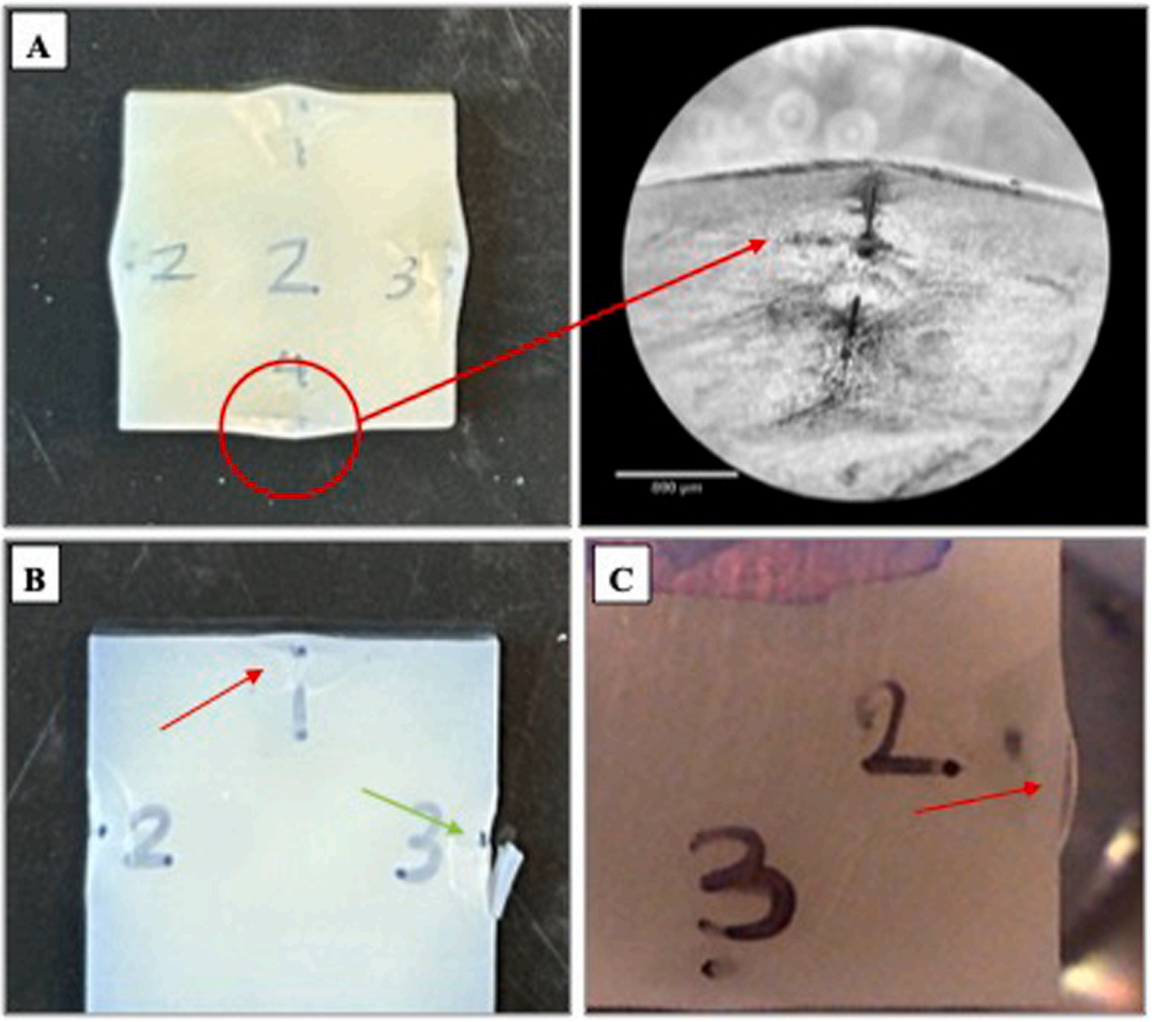

Fig. 2. (A) TC specimen after edge testing at 0.5 mm. Deep indentation and bulging of the edge are clearly noted. (B) A close up of one of the edges under optical microscope (×4) showing no cracks. (C) DT specimen after edge testing at 0.5 mm. Red arrow shows indentation and deformation of the edge. Green arrow shows incomplete chipping. (D) ND specimen after edge testing at 0.5 mm. Deep indentation and bulging is observed.

Table 3
Means and standard deviations of edge strength (N) for the different materials 0.5 mm and 1 mm from the edge.

	Material	Orientation	Edge strength at 0.5 mm (Dry)	Edge strength at 0.5 mm (48 h in AS)	Edge strength at 1 mm (48 h in AS)
3D-printed	VCP	0	161.9 (44.9)^{a}	109.4 (12.7)^{a}	
		45	201 (77.3)^{a}	111.2 (25.23)^{a}	
		90	243.1 (97.4)^{a,1}	318.2 (77.2)^{b,1,A}	484.2 (37.2)^{2A}
	CT	0	316.7 (133.9)^{a}	105.5 (10.9)^{a}	
		45	214.2 (57.3)^{a}	123.1 (18.9)^{a}	
		90	312.1 (159.6)^{a,1}	308.6 (92.5)^{b,1,A}	503.1 (59.9)^{2A}
Milled	LU		158.0 (43.4)^{1}	146.7 (24.7)^{1,B}	505.6 (117.3)^{2A}

The same superscript small letter within a column denotes non-significant differences between orientations of the same material and storage condition. The same superscript capital letter within a column denotes non-significant differences between materials. The same superscript number within a row denotes non-significant differences in a row.

For the LU group, the predominant failure mode was chipping, characterized by a single clean chip that did not affect the rest of the specimen (Fig. 7A). Fracture involved the specimen breaking in half and occurred mostly at 1 mm distance from the edge.

3.3. Filler content (wt%)

Table 4 presents the measured filler weight percentage for all the examined materials compared to the manufacturer-provided information. The filler weight percentage exhibited statistically significant differences in the following order: LU > CT ≥ VCP ($P < 0.05$). The filler weight percentages of VCP and CT were similar ($P = 0.9$). A non-significant negative correlation was observed between filler load and edge strength (r = -0.161, $P < 0.680$).

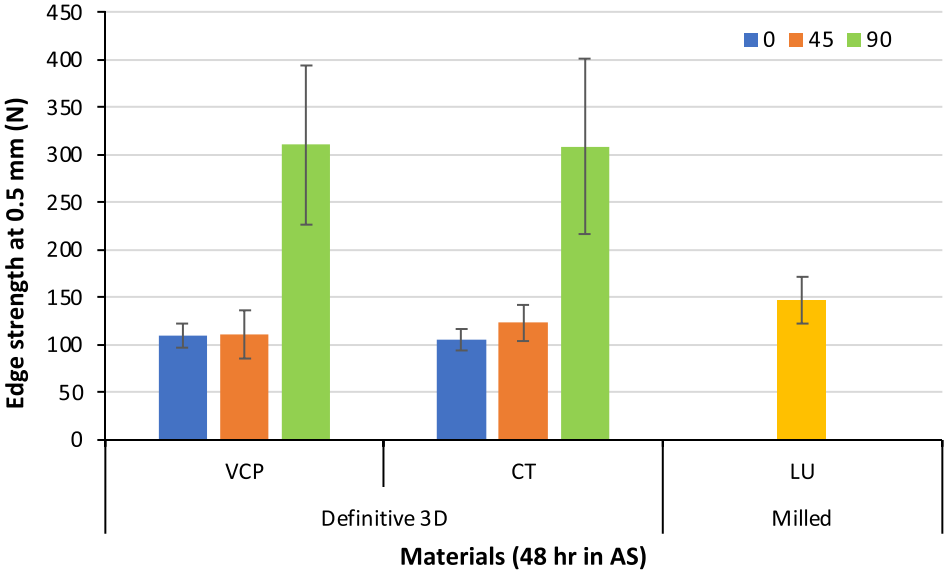

Fig. 3. Edge strength at 0.5 mm.

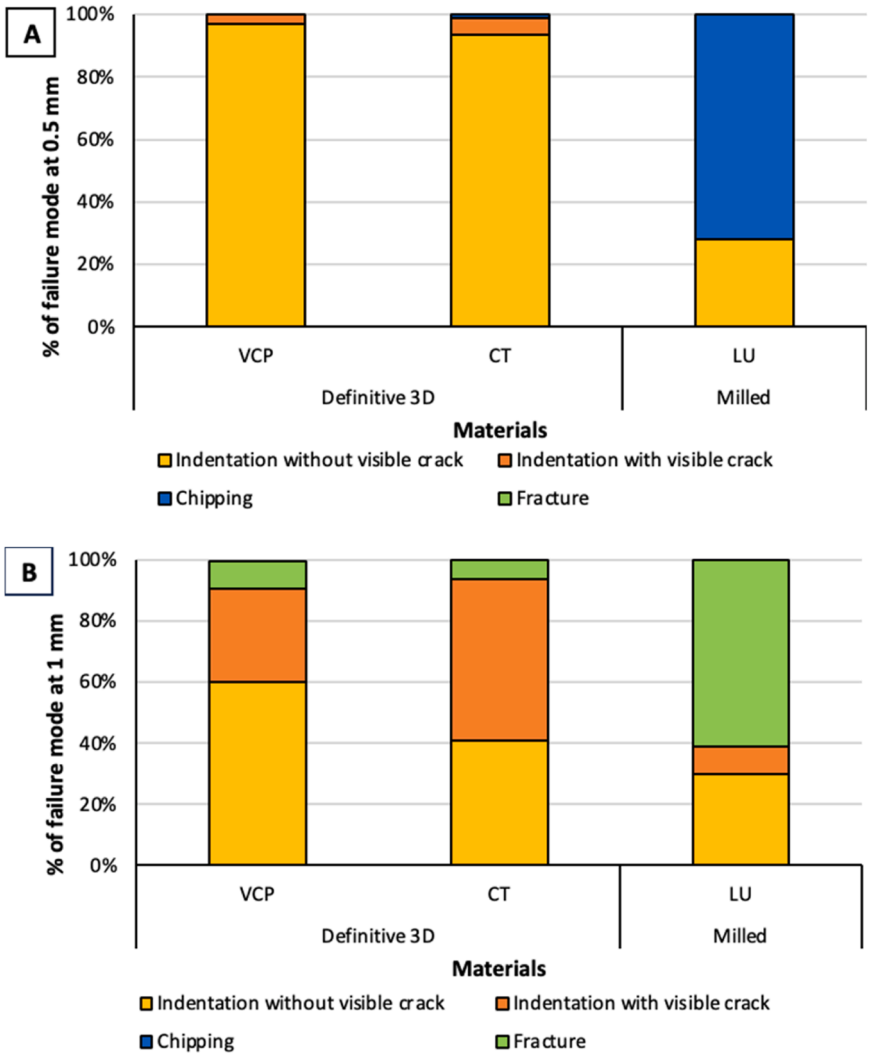

Fig. 4. Distribution percentage of failure modes at (A) 0.5 mm and (B) 1 mm from the edge.

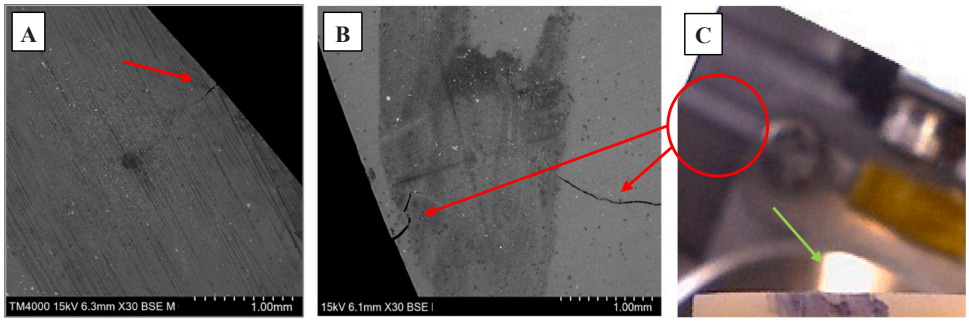

Fig. 5. Shallow indentation and cracks visible only under SEM × 30 (red arrows) (A) VCP (0.5 mm) (B) CT (1 mm) (C) Indentation with visible crack and bulging of the edge from plastic deformation (green arrow).

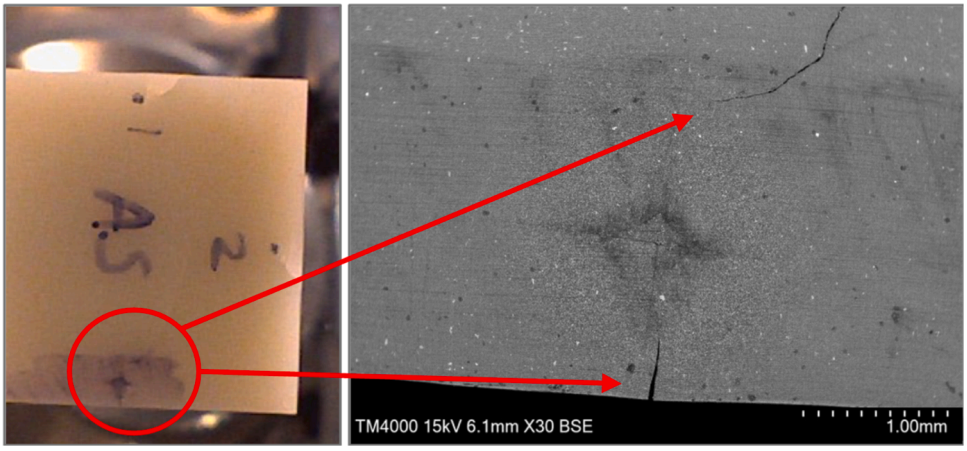

Fig. 6. Images of CT (1 mm) showing indentation with visible cracks (SEM × 30).

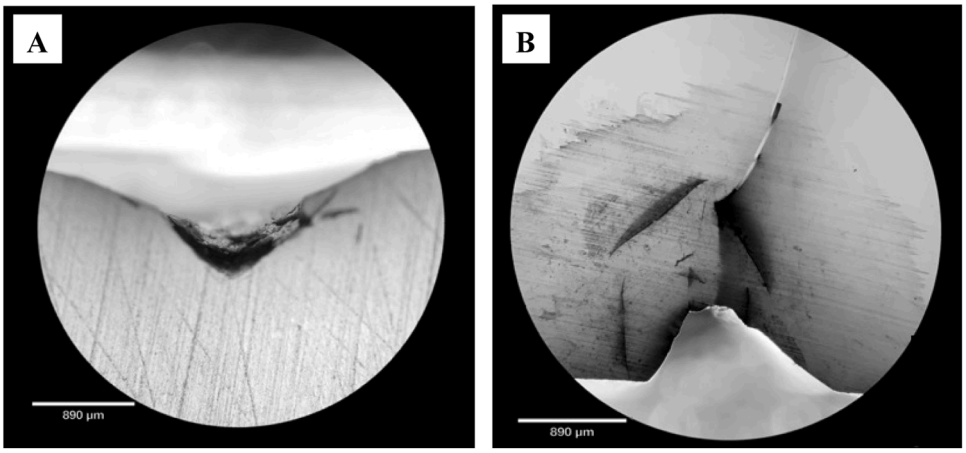

Fig. 7. Optical microscope images of edge chipping at 0.5 mm. (A) LU, (B) CT. Magnification 4 × , scale bar = 890 µm.

Table 4
Mean and standard deviation values for filler content wt% of all studied materials measured using the ash method (n = 3).

Category	Material	Manufacturer filler wt%	Measured filler wt%
3D-Printed	**VCP**	30–50	33.8 (0.3)[b]
	CT	30–50	33.4 (1.9)[b]
Milled	**LU**	80	73.5 (1.3)[a]

Different superscript letters denote significant variations between materials ($P \leq .05$)

4. Discussion

This study aimed to determine the edge strength of various aesthetic dental materials produced by 3D printing in various printing orientations. The results showed that the 90- degree printed specimens of the definitive materials had statistically higher edge forces than those of the 0- and 45 degrees. Thus, the 1st null hypothesis was partially accepted. Significant differences were observed in the ES between 3D printed and milled definitive materials. Thus the 2nd null hypothesis was partially accepted. The force required to create a chip increased with increasing distance from the edge, thus the 3rd null hypothesis was rejected. A non-

significant negative correlation between filler weight and ES was noted, thus the 3rd null hypothesis was accepted.

Many studies have evaluated various distances from the edge (0.5, 0.6, 0.7, 0.8, 0.9, 1 mm) to assess structural behaviour of different materials, consistently concluding that the force required to create a chip increases linearly with increasing distance from the edge [20,21, 25–27,30,32]. However, nonlinear behaviour has also been observed, particularly in soft dental restorative materials chipped with sharp indenters [33]. In this study, an additional 1 mm distance was chosen to confirm this relationship and was performed on a different set specimens printed at 90 degrees. This orientation was chosen because it showed higher ES in the definitive materials and also showed higher flexural strength and hardness [15,34]. The critical load causing failure did indeed increase for all materials when the distance was increased to 1 mm, indicating that edge-fracture resistance of resin composites is lower towards the margins of the restoration than towards the centre [21].

The specimen dimensions of 14 × 14 × 2 mm was selected to ensure all specimens were the same size, as the control materials are provided in the form of 14 × 14 mm blocks. Although previous studies using similar methodologies to test edge strength have employed different specimen dimensions, including disc-shaped [26] and rectangular-shaped specimens [30], the shape of the specimens is not expected to affect the results.

Specimen thickness is considered a key factor influencing fracture strength [20]. A thickness of 1 mm may be susceptible to deep indentations exceeding 100 μm, potentially compromising the material's ability to withstand stress and leading to premature failure [20]. Additionally, thinner specimens increase the likelihood of cracks and chips extending through the entire test piece, potentially invalidating the results [35]. Clinically, fixed partial denture preparation varies from 0.8 to 2 mm, depending on the type of restoration (crown, veneer, inlay), the restorative material (metal, metal-ceramic, all-ceramic, resin-based) [36,37], and the vitality of the tooth [38]. To ensure reliable testing and facilitate material comparisons, a standardized specimen thickness of 2 mm was selected. Literature also reports thicknesses of 2–2.5 mm in edge strength studies [26,39].

Differences in edge force between orientations were noted for VCP and CT, with this deference being evident after 48 hours of storage in AS where the 90-degree specimens exhibited higher edge force than those of the 0 and 45, although, there was no difference in their indentation failure mode. This is possibly attributed to the effect of aqueous storage on microstructure of the specimens. The 90-degree specimens were not severely affected by storage in AS compared to dry specimens, thus indicating a strong polymer network. Whereas the 0- and 45-degree orientations were significantly affected. A stronger polymer network in the 90-degree specimens could be either due to a higher degree of conversion during printing [40] or increased monomer conversion and cross linking reaction induced by elevated storage temperature [9,41]. Similar findings were reported by Zadeh et. al where the edge chipping resistance of different composite resins increased after water storage [42]. To the authors' knowledge, to-date only two other studies have evaluated the edge strength of 3D printed resins but did not evaluate the effect of orientation. Greil, Mayinger [43] printed their specimens in a vertical orientation (90 degrees) while Chung, Park [44] printed anatomical crowns in an angled orientation but the degree of angulation was not specified.

The 3D-printed and milled interim materials displayed significant edge deformation and bulging, with minimal chipping observed, consistent with findings from other studies on the edge strength of provisional materials [25]. This deformation is primarily attributed to their lower elastic modulus due to reduced filler weight. Materials with lower filler weight generally have decreased hardness and elastic modulus, making them softer and more flexible. This increased flexibility allows them to absorb stresses internally, making them more susceptible to plastic deformation [45,46]. Although the filler weight did not corelate significantly with ES, Quinn et al. [27] observed a negative correlation between hardness and edge toughness in dental composite resins: as material hardness increases, its resistance to chipping decreases. Supporting this, another study found that LU exhibited higher edge strength than more brittle and rigid ceramic materials with greater filler weight and elastic modulus [22].

The 3D-printed definitive materials demonstrated higher edge strength and greater resistance to chipping at a 0.5 mm distance compared to milled LU. Indentation and cracking were the primary failure modes, with minimal edge chipping observed. In contrast, LU displayed sudden edge chipping with an audible snap and minimal plastic deformation, likely due to differences in elasticity. The milled LU's greater elastic modulus renders it harder and stiffer than the 3D-printed materials [15]. Studies indicate that when a hard indenter applies pressure to a brittle surface, the material undergoes both plastic deformation and cracking, with greater plasticity leading to more indentation and less cracking. Simply put, softer materials produce larger indentations and consume more energy in plastic deformation under a given force [33,47], as observed in the 3D-printed materials (Fig. 5C). Additionally, another study found that LU exhibited higher edge strength than more brittle and rigid ceramic materials with greater filler weight and elastic modulus [22]. Consistent with this study, other research suggests that filler content in composite resins may not directly correlate with edge strength [19,21,42], as factors such as filler type, size, distribution, and particle matrix adhesion [48] play a more significant role in stress distribution and resistance to crack propagation [42,49,50].

Resin-based dental materials also exhibit viscoelastic behaviour, resulting in a time-dependent stress response that could prevent the sensor of the CK 10 machine from detecting non-brittle cracks, allowing for plastic deformation before cracking, Similar findings have been reported where the indenter remained in contact with the test piece after cracking causing additional damage and a larger indentation [27,35].

Compositional and microstructural complexities also contribute to differences between materials [30]. Kim and Watts et al. [25] evaluated the edge strength of monomethacrylates and dimethylmethacrylate in polymer-based provisional crown and bridge materials. They found that monomethacrylates experienced lateral deformation without chipping due to molecular movement under stress, while dimethacrylates chipped at certain distances, likely due to their more resistant three-dimensional network structure. In this study, LU had different dimethacrylates in its composition which might explain the more edge chipping observed at 0.5 than the 3D printed materials which their composition is not fully disclosed.

Benetti et al. [51] reported a higher incidence of fracture near the margin in resin materials with a higher elastic modulus, aligning with findings at 0.5 mm from the edge in this study. However, as the distance from the edge increased to 1 mm, no difference was observed between the definitive 3D-printed and milled materials. This can be explained by the increased material bulk, improved load distribution, and reduced stress concentration at greater distances from the edge, along with fewer surface and machining defects [52]. However, at a 1 mm distance, fracture failures were more prevalent in the LU group, often involving the entire sample. Clinically, such failures in LU could lead to significant consequences, making restoration replacement inevitable. Conversely, the 3D-printed group showed indentation with visible cracks. If such failures occur clinically, they may not necessitate restoration replacement and could be monitored or even repaired as needed [30].

Mechanical properties of resin composites are reduced after aging and determining edge force after wet storage might therefore be a clinically relevant supplement. All groups, except for VCP (90-degree), showed a decrease in ES after aqueous storage which is linked to solvent infiltration into the resin matrix, leading to swelling and plasticization, dislodgment of fillers, and the release of unreacted components, all of which reduce the mechanical properties [53]. This finding is in line with many studies evaluating the mechanical properties of resin materials

after aqueous storage [43,54,55]. However, VCP (90-degree) showed an increase in ES which might be linked to increased monomer conversion and cross-linking reaction induced by elevated storage temperature [9,41].

Overall, the 3D-printed resins exhibited greater susceptibility to aging compared to the milled LU. This may be attributed to the fabrication process of resin composite blocks in subtractive manufacturing, where they are polymerized under controlled temperatures and high pressure. This method enhances the degree of conversion, strengthens mechanical properties, and ensures a more uniform structure with minimal flaws and porosity compared to traditional manufacturing techniques [56,57]. In contrast, DLP 3D-printed restorations are produced through layer-by-layer polymerization of photosensitive resins using light emitted from the printer [58]. To optimize polymerization and improve mechanical performance, manufacturers recommend additional post-printing light exposure, with or without heat, depending on the material [59]. This variation in fabrication methods may contribute to differences in polymer networks, influencing material stability in an aqueous environment [15].

While edge strength tests provide valuable data on material performance, their clinical relevance can be limited. The testing conditions often do not fully replicate the complex oral environment, which includes factors like temperature fluctuations and cyclic loading. Different materials exhibit distinct failure modes, such as chipping or cracking, which can affect the interpretation of edge strength. Understanding these failure modes is crucial for translating laboratory results to clinical scenarios.

5. Conclusions

Based on the findings of the study, the following can be concluded:

1. 3D printing definitive resin materials at a 90-degree orientation provided increased edge strength.
2. 3D printed materials showed minimal chipping and cracking compared to milled composites.
3. Increased filler weight did not improve edge strength.

Declaration of Competing Interest

The authors declare that they have no conflicts of interest related to the publication of this research.

Acknowledgements

The first author (Shaymaa Mudhaffer) was funded by a full-time scholarship by the Saudi Arabian Cultural Bureau in London, UK.

References

[1] Christina H, Maria B, Athina B, Petros K. 3D printing in dentistry with emphasis on prosthetic rehabilitation and regenerative approaches. 3D Printing: Applications in Medicine and Surgery Volume 2. Elsevier; 2022. p. 195–219.
[2] Alzahrani SJ, Hajjaj MS, Azhari AA, Ahmed WM, Yeslam HE, Carvalho RM. Mechanical properties of three-dimensional printed provisional resin materials for crown and fixed dental prosthesis: a systematic review. Bioeng (Basel) 2023;10:663.
[3] Alharbi A, Ardu S, Bortolotto T, Krejci I. Stain susceptibility of composite and ceramic CAD/CAM blocks versus direct resin composites with different resinous matrices. Odontology 2017;105:162–9.
[4] Tahayeri A, Morgan M, Fugolin AP, Bompolaki D, Athirasala A, Pfeifer CS, et al. 3D printed versus conventionally cured provisional crown and bridge dental materials. Dent Mater 2018;34:192–200.
[5] Kessler A, Hickel R, Reymus M. 3D printing in dentistry—State of the art. Oper Dent 2020;45:30–40.
[6] Lee BI, You SG, You SM, Kim DY, Kim JH. Evaluating the accuracy (trueness and precision) of interim crowns manufactured using digital light processing according to post-curing time: an in vitro study. J Adv Prosthodont 2021;13:89–99.
[7] Zohdi N, Yang R. Material anisotropy in additively manufactured polymers and polymer composites: a review. Polymers 2021;13:3368.
[8] Väyrynen VO, Tanner J, Vallittu PK. The anisotropicity of the flexural properties of an occlusal device material processed by stereolithography. J Prosthet Dent 2016;116:811–7.
[9] Reymus M, Fabritius R, Keßler A, Hickel R, Edelhoff D, Stawarczyk B. Fracture load of 3D-printed fixed dental prostheses compared with milled and conventionally fabricated ones: the impact of resin material, build direction, post-curing, and artificial aging—an in vitro study. Clin Oral Invest 2020;24:701–10.
[10] Espinar C, Della Bona A, Tejada-Casado M, Pulgar R, Pérez MM. Optical behavior of 3D-printed dental restorative resins: influence of thickness and printing angle. Dent Mater 2023;39:894–902.
[11] Revilla-León M, Jordan D, Methani MM, Piedra-Cascón W, Özcan M, Zandinejad A. Influence of printing angulation on the surface roughness of additive manufactured clear silicone indices: an in vitro study. J Prosthet Dent 2021;125:462–8.
[12] Al-Dulaijan YA, Alsulaimi L, Alotaibi R, Alboainain A, Alalawi H, Alshehri S, et al. Comparative evaluation of surface roughness and hardness of 3D printed resins. Materials 2022;15:6822.
[13] Hickel Kessler A, Ilie R. In vitro investigation of the influence of printing direction on the flexural strength, flexural modulus and fractographic analysis of 3D-printed temporary materials. Dent Mater J 2021;40:641–9.
[14] Turksayar AAD, Donmez MB, Olcay EO, Demirel M, Demir E. Effect of printing orientation on the fracture strength of additively manufactured 3-unit interim fixed dental prostheses after aging. J Dent 2022;124:104155.
[15] Mudhaffer S, Althagafi R, Haider J, Satterthwaite J, Silikas N. Effects of printing orientation and artificial ageing on martens hardness and indentation modulus of 3D printed restorative resin materials. Dent Mater 2024;40:1003–14.
[16] de Castro EF, Nima G, Rueggeberg FA, Giannini M. Effect of build orientation in accuracy, flexural modulus, flexural strength, and microhardness of 3D-printed resins for provisional restorations. J Mech Behav Biomed Mater 2022;136:105479.
[17] Brandeburski SBN, Vidal ML, Collares K, Zhang Y, Della Bona A. Edge chipping test in dentistry: a comprehensive review. Dent Mater 2020;36:e74–84.
[18] Chai H, Lawn BR. A universal relation for edge chipping from sharp contacts in brittle materials: a simple means of toughness evaluation. Acta Mater 2007;55:2555–61.
[19] Lohbauer U, Belli R, Cune MS, Schepke U. Fractography of clinically fractured, implant-supported dental computer-aided design and computer-aided manufacturing crowns. SAGE Open Med Case Rep 2017;5:2050313X17741015.
[20] Pfeilschifter M, Preis V, Behr M, Rosentritt M. Edge strength of CAD/CAM materials. J Dent 2018;74:95–100.
[21] Baroudi K, Silikas N, Watts DC. Edge-strength of flowable resin-composites. J Dent 2008;36:63–8.
[22] Hampe R, Theelke B, Lümkemann N, Stawarczyk B. Impact of artificial aging by thermocycling on edge chipping resistance and Martens hardness of different dental CAD-CAM restorative materials. J Prosthet Dent 2021;125:326–33.
[23] Ilie N, Hilton TJ, Heintze SD, Hickel R, Watts DC, Silikas N, et al. Academy of dental materials guidance—resin composites: part i—mechanical properties. Dent Mater 2017;33:880–94.
[24] Quinn G. On edge chipping testing and some personal perspectives on the state of the art of mechanical testing. Dent Mater 2015;31:26–36.
[25] Kim SH, Watts DC. In vitro study of edge-strength of provisional polymer-based crown and fixed partial denture materials. Dent Mater 2007;23:1570–3.
[26] Watts DC, Issa M, Ibrahim A, Wakiaga J, Al-Samadani K, Al-Azraqi M, et al. Edge strength of resin-composite margins. Dent Mater 2008;24:129–33.
[27] Quinn G, Giuseppetti A, Hoffman K. Chipping fracture resistance of denture tooth materials. Dent Mater 2014;30:545–53.
[28] Fusayama T, Katayori T, Nomoto S. Corrosion of gold and amalgam placed in contact with each other. J Dent Res 1963;42:1183–97.
[29] El Mallakh B, Sarkar N. Fluoride release from glass-ionomer cements in de-ionized water and artificial saliva. Dent Mater 1990;6:118–22.
[30] Ereifej N, Silikas N, Watts DC. Edge strength of indirect restorative materials. J Dent 2009;37:799–806.
[31] ISO-1172. Textile-Glass-Reinforced Plastics—Prepregs, Moulding Compounds and Laminates—Determination of the Textile-Glass and Mineral-Filler Content Using Calcination Methods. Geneva, Switzerland: International Organization for Standardization 1999.
[32] Zakiev I, Storchak M, Gogotsi GA, Zakiev V, Kokoieva Y. Instrumented indentation study of materials edge chipping. Ceram Int 2021;47:29638–45.
[33] Quinn G, Giuseppetti A, Hoffman K. Chipping fracture resistance of dental CAD/CAM restorative materials: Part 2. Phenomenological model and the effect of indenter type. Dent Mater 2014;30:e112–23.
[34] Mudhaffer S, Haider J, Satterthwaite J, Silikas N. Effects of print orientation and artificial aging on the flexural strength and flexural modulus of 3D printed restorative resin materials. J Prosthet Dent 2024.
[35] Quinn G, Giuseppetti A, Hoffman K. Chipping fracture resistance of dental CAD/CAM restorative materials: Part I–Procedures and results. Dent Mater 2014;30:e99–111.
[36] Blair FM, Wassell RW, Steele JG. Crowns and other extra-coronal restorations: preparations for full veneer crowns. Br Dent J 2002;192. 561-4, 7-71.
[37] Goodacre CJ, Campagni WV, Aquilino SA. Tooth preparations for complete crowns: an art form based on scientific principles. J Prosthet Dent 2001;85:363–76.
[38] Homsy F, Eid R, El Ghoul W, Chidiac JJ. Considerations for altering preparation designs of porcelain inlay/onlay restorations for nonvital teeth. J Prosthodont 2015;24:457–62.
[39] Argyrou R, Thompson GA, Cho S-H, Berzins DW. Edge chipping resistance and flexural strength of polymer infiltrated ceramic network and resin nanoceramic restorative materials. J Prosthet Dent 2016;116:397–403.

[40] Altarazi A, Haider J, Alhotan A, Silikas N, Devlin H. Assessing the physical and mechanical properties of 3D printed acrylic material for denture base application. Dent Mater 2022;38:1841–54.
[41] De Moraes RR, Marimon JLM, Jochims Schneider LF, Sinhoreti MAC, Correr-Sobrinho L, Bueno M. Effects of 6 months of aging in water on hardness and surface roughness of two microhybrid dental composites. J Prosthodont 2008;17:323–6.
[42] Zadeh PN, Stawarczyk B, Hampe R, Liebermann A, Mayinger F. Edge chipping resistance of veneering composite resins. J Mech Behav Biomed Mater 2021;116:104349.
[43] Greil V, Mayinger F, Reymus M, Stawarczyk B. Water sorption, water solubility, degree of conversion, elastic indentation modulus, edge chipping resistance and flexural strength of 3D-printed denture base resins. Mech Behav Biomed Mater 2023;137:105565.
[44] Chung YJ, Park JM, Kim TH, Ahn JS, Cha HS, Lee JH. 3D printing of resin material for denture artificial teeth: chipping and indirect tensile fracture resistance. Materials 2018;11:1798.
[45] Haak R, Wicht MJ, Noack MJ. Marginal and internal adaptation of extended class I restorations lined with flowable composites. J Dent 2003;31:231–9.
[46] Comba A, Scotti N, Maravić T, Mazzoni A, Carossa M, Breschi L, et al. Vickers hardness and shrinkage stress evaluation of low and high viscosity bulk-fill resin composite. Polymers 2020;12:1477.
[47] Morrell R, Gant A. Edge chipping of hard materials. Int J Refract Met Hard Mater 2001;19:293–301.
[48] Manhart J, Kunzelmann K, Chen H, Hickel R. Mechanical properties and wear behavior of light-cured packable composite resins. Dent Mater 2000;16:33–40.
[49] Masouras K, Silikas N, Watts DC. Correlation of filler content and elastic properties of resin-composites. Dent Mater 2008;24:932–9.
[50] Ornaghi BP, Meier MM, Lohbauer U, Braga RR. Fracture toughness and cyclic fatigue resistance of resin composites with different filler size distributions. Dent Mater 2014;30:742–51.
[51] Benetti AR, Peutzfeldt A, Lussi A, Flury S. Resin composites: modulus of elasticity and marginal quality. J Dent 2014;42:1185–92.
[52] Lardner T, Ritter J, Shiao M, Lin M. Behavior of indentation cracks near free surfaces and interfaces. Int J Fract 1990;44:133–43.
[53] Ferracane JL. Hygroscopic and hydrolytic effects in dental polymer networks. Dent Mater 2006;22:211–22.
[54] Egilmez F, Ergun G, Cekic-Nagas I, Vallittu PK, Lassila LV. Does artificial aging affect mechanical properties of CAD/CAM composite materials. J Prosthodont Res 2018;62:65–74.
[55] Gad MM, Fouda SM. Factors affecting flexural strength of 3D-printed resins: a systematic review. J Prosthodont 2023;32:96–110.
[56] Balkenhol M, Mautner MC, Ferger P, Wöstmann B. Mechanical properties of provisional crown and bridge materials: chemical-curing versus dual-curing systems. J Dent 2008;36:15–20.
[57] Nguyen JF, Migonney V, Ruse ND, Sadoun M. Resin composite blocks via high-pressure high-temperature polymerization. Dent Mater 2012;28:529–34.
[58] Dos Santos G, Alto RM, Sampaio Filho H, Da Silva E, Fellows C. Light transmission on dental resin composites. Dent Mater 2008;24:571–6.
[59] Vitale A, Cabral JT. Frontal conversion and uniformity in 3D printing by photopolymerisation. Materials 2016;9:760.